EVS26
Los Angeles, California, May 6-9, 2012

Variability of Battery Wear in Light Duty Plug-In Electric Vehicles Subject to Ambient Temperature, Battery Size, and Consumer Usage

Eric Wood, Jeremy Neubauer, Aaron D. Brooker, Jeffrey Gonder, and Kandler A. Smith
National Renewable Energy Laboratory, Center for Transportation Technologies and Systems
1617 Cole Blvd., Golden, CO 80401, U.S.A.
eric.wood@nrel.gov

Abstract

Battery wear in plug-in electric vehicles (PEVs) is a complex function of ambient temperature, battery size, and disparate usage, and is not well understood. Battery life simulation scenarios that capture varying ambient temperature profiles, battery sizes, and driving patterns are of great value to battery manufacturers and vehicle original equipment manufacturers. This study seeks to improve understanding of battery wear in PEVs by implementing a predictive battery wear model, developed by the National Renewable Energy Laboratory, that is capable of capturing the effects of multiple cycling and storage conditions in a representative lithium chemistry. In particular, this paper explores the sensitivity of battery wear rates to ambient conditions, maximum allowable depth of discharge, and vehicle miles traveled. The analysis focuses on two midsize vehicle platforms: a battery electric vehicle (BEV) with a nominal range of 75 mi (121 km) and a plug-in hybrid electric vehicle (PHEV) with 40 mi (64 km) of nominal charge-depleting range. Current U.S. hybrid electric vehicle populations are used to focus analysis on markets where consumers have shown a tendency towards early adoption of advanced vehicle technology. Both cross-sectional and longitudinal driving distance distributions are implemented to represent the variability of vehicle use, both vehicle-to-vehicle and day-to-day. In the scenarios examined, battery wear over an 8-year period was found to be dominated by ambient conditions for the BEV with capacity fade ranging from 19% to 32% while the PHEV was most sensitive to maximum allowable depth of discharge with capacity fade ranging from 16% to 24%. In addition, the BEV and PHEV were found to be comparable in terms of petroleum displacement potential after 8 years of service due to the BEV's limited utility for accomplishing long trips. Future work may include incorporating the effects of temperature on pack internal resistance/available capacity and analyzing a range of vehicle-to-grid scenarios.

Keywords: lithium battery, battery calendar life, cycle life, BEV, PHEV

1 Introduction

Plug-in electric vehicles (PEVs) are an advanced vehicle technology capable of reducing liquid petroleum consumption by storing and using energy from the electric grid in an on-board battery. Widespread adoption of PEVs will be impacted by the ability of original equipment

manufacturers to accurately predict battery life to produce durable vehicles at a reasonable price. Unfortunately, battery life in PEVs is inherently variable with factors such as ambient temperature, vehicle miles traveled (VMT), and charging behavior all interacting to produce potentially disparate power and energy fade rates. Battery wear is also sensitive to maximum allowable depth of discharge (DoD) and pack thermal management. The degree to which these sizing and usage conditions impact battery wear rates and the variability of wear rates is explored.

2 Project Approach

To explore the sensitivity and variability of battery wear rate in PEVs to various parameters, a predictive battery wear model developed by the National Renewable Energy Laboratory (NREL) was implemented [1]. The life model is informed by vehicle powertrain and battery pack thermal modeling capabilities developed internally at NREL. By leveraging these existing capabilities, it was possible to capture the effects of drive cycle-based loading and ambient conditions on battery wear rates in a predictive and robust method. An overview of this integrated approach is provided, followed by an explanation of various sizing and usage scenarios examined.

2.1 Battery Life Model

Battery aging is caused by multiple phenomena related to both cycling and calendar age. Battery degradation is accelerated with the DoD of cycling, elevated temperature, and elevated voltage exposure, among other factors. At the battery terminals, the observable effects of degradation are an increase in resistance and a reduction in capacity. These two effects can be correlated with power and energy loss that cause battery end-of-life in an application. Mechanisms for resistance growth include loss of electrical conduction paths in the electrodes, fracture and isolation of electrode sites, growth of film layers at the electrode surface, and degradation of the electrolyte. Mechanisms for capacity loss include fracture, isolation, and chemical degradation of electrode material, as well as loss of cyclable lithium (Li) from the system as a byproduct of side reactions.

Under storage or calendar-aging conditions, the dominant fade mechanism is typically growth of a resistive film layer at the electrode surface. As the layer grows, cyclable Li is also consumed from the system, reducing capacity. In the present model, resistance growth and Li-capacity loss are assumed to be proportional to the square-root of time, $t^{1/2}$, typical of diffusion-limited film-growth processes [2]. Under cycling-intense conditions, degradation is mainly caused by structural degradation of the electrode matrix and active sites. Cycling-driven degradation is assumed to be proportional to the number of cycles, *N*. Cell resistance growth due to calendar- and cycling-driven mechanisms are assumed to be additive:

$$R = a_o + a_1 t^{1/2} + a_2 N \quad (1)$$

Cell capacity is assumed to be controlled by either loss of cyclable Li or loss of electrode sites,

$$Q = \min(Q_{Li}, Q_{sites}) \quad (2)$$

where

$$Q_{Li} = b_o + b_1 t^{1/2} \quad (3)$$

$$Q_{sites} = c_o + c_1 N \quad (4)$$

Models (1), (3), and (4) are readily fit to a resistance or capacity trajectory measured over time for one specific storage or cycling condition. Using multiple storage and cycling datasets, functional dependence can be built for rate constants $a_i(T, V, DoD)$, $a_2(T, V, DoD)$, $b_i(T, V, DoD)$, and $c_i(T, V, DoD)$. The present battery life model was fit to laboratory aging datasets [3]–[6] for the Li-ion graphite/nickel-cobalt-aluminum (NCA) chemistry as described in [6]. The graphite/NCA chemistry has generally graceful aging characteristics and is expected to achieve 8 or more years of life when sized appropriately for a vehicle application.

The life model employed in this analysis was matched to experimental data for a graphite/NCA Li-ion cell with up to 25% battery capacity fade. Beyond this level of wear, fade rates may accelerate, as sometimes evidenced in experimental data by a sharp drop in remaining capacity with continued cycling. The present life model does not capture possible accelerating fade mechanisms that could occur beyond 25% capacity fade.

In addition, the life model has been shown to have weak sensitivity to normal battery temperature variation over the course of a single day, particularly when the thermal mass of the battery is taken into account [7]. As such, this analysis uses

average monthly temperatures as inputs to the life model to capture the effect of seasonal variability in disparate climate regions of the United States.

While high heat generation rates resulting from aggressive driving are correlated to increased battery temperature, the impact of fast charging as it relates to rate-induced wear is not considered in the present model.

2.2 FASTSim Vehicle Model

Vehicle modeling was performed using a high-level tool developed at NREL known as FASTSim (Future Automotive Systems Technology Simulator). The analysis focuses on two midsize vehicle platforms: a battery electric vehicle (BEV) with a nominal range of 75 mi (121 km) and a plug-in hybrid electric vehicle (PHEV) with 40 mi (64 km) of nominal charge-depleting (CD) range followed by charge-sustaining (CS) operation via a gasoline-fueled internal combustion engine. Table 1 summarizes the platform and component parameters selected for the BEV and PHEV models, which are roughly similar to the configuration of the production Nissan Leaf and Chevrolet Volt, respectively [8]–[9].

Table 1. FASTSim vehicle model inputs (baseline values).

	BEV	PHEV
Drag Coefficient (C_d)	0.29	0.28
Frontal Area (m^2)	2.27	2.13
Vehicle Mass (kg)	1663	1850
Engine Power (kW)	NA	53
Battery Capacity (kWh)	24	16
Maximum SOC	95%	85%
Maximum Allowable DoD	90%	65%
Battery Thermal Management System	No active cooling	Liquid cooling
Accessory Load (W)	300	300
Approx UDDS CD Range (mi)	100	50
Approx Adjusted CD Range (mi)	75	40

Battery internal heat generation rates were correlated with drive cycles through vehicle simulations informed with cell-level test data for a representative Li chemistry. Nominal heat generation rates were determined using the California Air Resources Board LA92 drive cycle, which was found to produce moderate heat generation rates characteristic of real-world drive cycles (see Table 2).

Table 2. Cycle attributes determined through simulation of BEV and PHEV.

Drive Cycle	Time, s	Distance, km	Avg Speed, km*hr^{-1}	BEV Avg Heat Gen, W	PHEV Avg Heat Gen, W
UDDS	1,369	11.99	31.5	60	103
LA92	1,435	15.80	39.6	152	232
US06	600	12.89	77.8	477	622

2.3 Vehicle Thermal Model

To correlate ambient conditions to battery temperature, a detailed thermal vehicle model was implemented. Based on previous analysis done by NREL on a Toyota Prius [10], the thermal model captures heating due to both ambient temperature profiles and solar loading (see Figure 1). These inputs are merged with battery internal heat generation profiles during driving and charging to calculate the average battery temperature over the course of a 24-hour period. In addition to passive heat transfer to ambient, the PHEV battery pack is equipped with an active thermal management system (TMS) capable of maintaining the battery temperature within a desired band when driven or plugged in. An active TMS was used to mitigate the effects of greater heat generation rates and smaller thermal mass in the PHEV pack whereas the modeled BEV employed passive thermal management. This methodology reflects current approaches of original equipment manufacturers and provides a means for evaluating different TMS strategies.

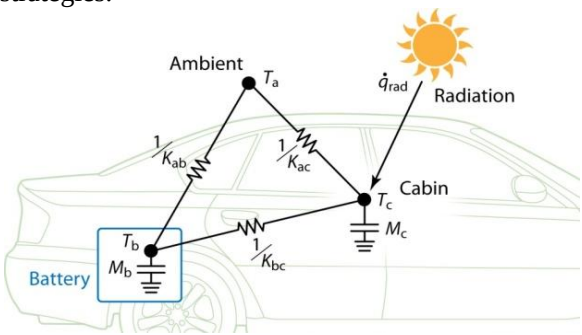

Figure 1. Vehicle thermal model employed to calculate battery temperature with respect to ambient temperature, solar loading, and thermal insulation.

Battery temperature was correlated to ambient for the passively cooled BEV in two steps (see Figure

2). First, an annual average battery temperature above ambient temperature in three different climates (shown in blue) was calculated according to the total solar loading for a given day (shown in green). In addition to solar loading, a second temperature differential was calculated as a result of battery heat generation and passive dissipation during driving and charging (shown in red). The temperature increase resulting from driving is a function of both daily driving distance and average ambient temperature.

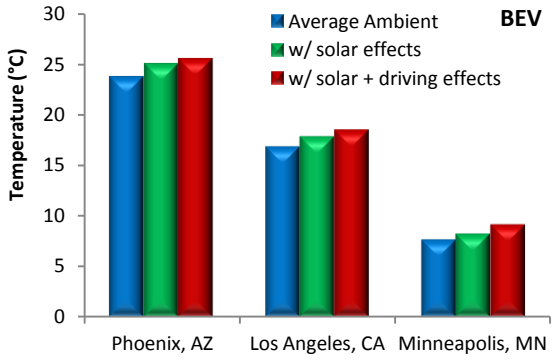

Figure 2. Average yearly battery temperature contributions from ambient, solar loading, and internal heat generation for simulated BEV.

Noticeably, contributions to average battery temperature from driving are relatively small, accounting for an increase of less than one degree Celsius in all climates. For the BEV, this can be attributed to both the large percentage of drive days with zero miles (approximately 16%) and the number of trips omitted due to distances greater than the range of the vehicle (see section 2.4.3).

Unlike for the BEV, contributions to battery temperature for the PHEV cannot be assumed to be additive due to the ability of the active TMS to heat or cool the battery as necessary. Contributions to battery temperature in the PHEV are attributed to three sources: (i) ambient temperature, (ii) solar loading and (iii) heat generation plus active cooling while driving/charging. A baseline battery temperature (shown in blue) is calculated as the difference above the ambient temperature due to solar loading (shown in Figure 3 in green). The red bar shows the adjusted temperature due to heat generated during driving/charging and the effects of the active TMS. The TMS is assumed to only operate when the vehicle is being driven or while plugged in. All scenarios assume that the PHEV is left unplugged and stationary (implying an inactive TMS) for approximately 8 hours during the course of the day.

While battery temperature calculations are performed to account for variations in driver aggression, active versus passive TMS, and daily distance, the cell-level effects of temperature on internal resistance and capacity are not captured in the present model. For example, a BEV battery pack in Minneapolis may experience significantly lower temperatures and subsequently reduced vehicle efficiency and range. In addition, auxiliary loading placed on the PHEV resulting from operation of the active TMS with the potential to limit CD range is not considered. Auxiliary climate control loading has the potential to significantly impact the CD range of PEVs as shown in [11]. Future battery wear analysis may address temperature effects on cell internal resistance and capacity to quantify the impact of active TMS on PEV efficiency and utility.

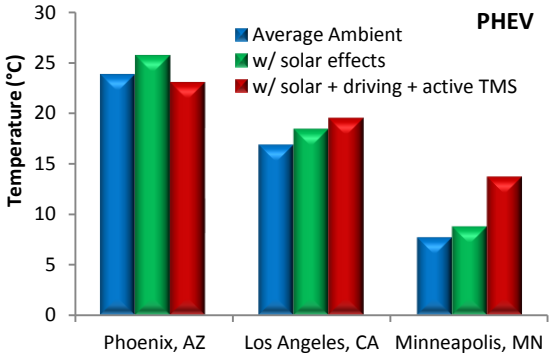

Figure 3. Average yearly battery temperature contributions from ambient, solar loading, active cooling, and internal heat generation for simulated PHEV.

2.4 Design of Experiments

Upon successful integration of the battery life model, the vehicle powertrain model, and the vehicle thermal model, the BEV and PHEV were run through a matrix of location, battery size, and usage scenarios with the primary outputs being battery resistance growth and capacity fade at 8 years. An initial sensitivity analysis revealed ambient conditions, maximum allowable DoD, and VMT to have the greatest influence on battery wear. The design of experiments used to study the effects of these variables is described in greater detail below.

2.4.1 U.S. Ambient Conditions

An expected distribution of wear rates was desired for both vehicles subject to U.S. ambient conditions. Current hybrid electric vehicle (HEV) population data were used as an estimate for the

future distribution of PEVs. HEV population statistics highlight both large markets and regions where consumers have shown a tendency towards early adoption of advanced vehicle technology. The Polk Company's 2010 light-duty vehicle registration dataset [12] was used to determine the top 100 U.S. metropolitan areas in terms of number of HEVs (see Figure 4). These locations account for approximately 75% of the total U.S. HEV population and represent a plausible estimate for the location distribution of PEV early adopters. Note from Table 3 moderate climates representative of the U.S. average.

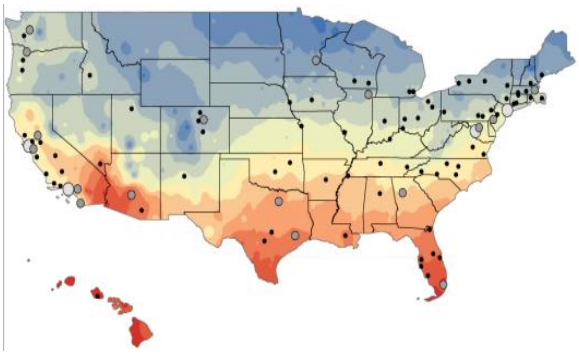

Figure 4. U.S. metropolitan areas with large HEV populations overlaid onto average ambient temperature map. (Credit: Evan Burton, NREL)

Table 3. Top five U.S. metropolitan areas in terms of HEV population.

Metropolitan Area	# of HEVs
Los Angeles, CA	149,042
New York City, NY	86,773
San Francisco, CA	82,756
Washington, DC	66,720
Chicago, IL	52,158

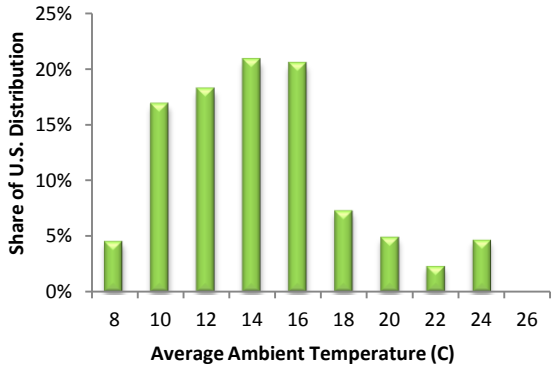

Figure 5. Weighted distribution of average ambient temperatures based on existing HEV populations.

Ambient temperature and solar irradiation data were assembled from NREL's Typical Meteorological Year Database (TMY3) [13]. The national weighted distribution of average yearly ambient temperatures can be seen in Figure 5. The TMY3 data were aggregated into monthly averages because hourly and daily battery temperature variations were shown to have a negligible effect on wear rates in the battery life model.

2.4.2 Depth of Discharge

The effect of maximum allowable DoD on battery wear is explored for both the BEV and the PHEV. Each vehicle was assigned a nominal value for maximum allowable DoD and maximum state of charge (SOC). These values are adjusted over a feasible range for both the BEV and PHEV to explore the effect on wear (80%–94% and 55%–87% maximum allowed DoD, respectively). The SOC window of the pack is adjusted relative to total energy to ensure that the available energy in the pack remains constant for all maximum allowable DoDs. By adjusting the maximum allowable DoD and maximum SOC, the life model will capture the wear effects of deep cycling and operation at high voltages.

Adjusting pack energy has an impact on vehicle mass (and cost) and is subsequently related to CD range, efficiency, and acceleration. In light of these interactions, the maximum allowable DoD was restricted to values that produced vehicle range, efficiency, and acceleration values within ±1% of the nominal design.

2.4.3 Vehicle Miles Traveled

This analysis uses fleet-aggregated driving distance statistics in addition to longitudinal (multi-day) travel profiles to represent the variability of travel behavior, both from vehicle to vehicle and from day to day. Fleet-aggregated statistics represent a snapshot of the travel patterns for a large fleet of vehicles on a given day. In this study, fleet-aggregated statistics are taken from the 2001 National Household Travel Survey (NHTS) [14] to reflect the behavior of the U.S. fleet. Using the NHTS, a distribution of fleet distances was created with a zero mile per day probability calculated as approximately 16% (about one day per week) such that the nominal VMT of the distribution was equal to 12,375 miles per year (19,916 km per year). This aggregated distribution is used as the default for analysis of ambient conditions and maximum allowable DoD.

To investigate the effect of VMT on battery wear, a large number of longitudinal distributions were simulated to capture the variable behavior of consumers. Longitudinal vehicle distributions track the driving behavior of individual vehicles over time and tend to exhibit a more focused set of distances with a small number of probability peaks representing routes frequently traveled. Figure 6 shows three examples of longitudinal profiles.

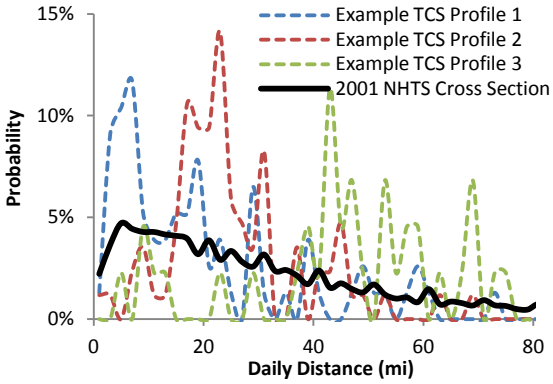

Figure 6. NHTS cross sectional distribution and three example longitudinal distributions taken from the Traffic Choices Study.

Longitudinal distributions used in this analysis are derived from the Puget Sound Regional Council's 2007 Traffic Choices Study (TCS) [15]. The TCS was an investigation of the response of travel behavior to variable toll charges in the Seattle metropolitan area. The study placed global positioning systems in 445 vehicles from 275 volunteer households that recorded driving patterns over an 18-month average per household period. The experiment started with a baseline period in which no artificial tolls were applied to affect behavior. We processed the data for use in this study by (i) only considering data collected during the approximately 3-month baseline period, (ii) eliminating vehicles for which no driving took place during the baseline period, (iii) eliminating vehicles for which significant errors in data recording were identified, and (iv) reducing detailed trip data to daily driving distance based upon the length of each trip and the date on which it was started. The resultant data were then converted into 398 longitudinal profiles of daily VMT with each profile representing one vehicle over multiple days. A distribution of annual VMT derived from this set of 398 longitudinal profiles is shown in Figure 7.

VMT calculations for the BEV do not include driving days where the expected daily distance is greater than the nominal vehicle range. This assumption represents a conservative, near-term outlook. Alternate scenarios considering distributed charging, DC fast charging, or battery swapping could reflect greater utility for the BEV.

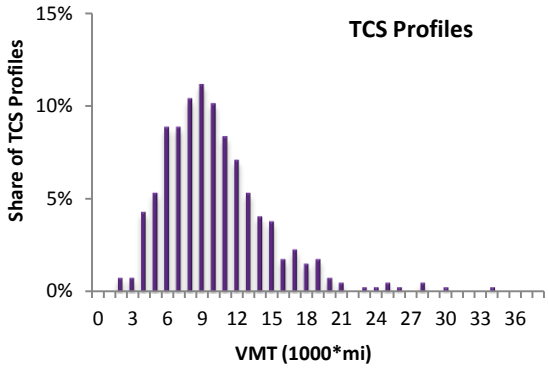

Figure 7. Distribution of annual VMT for 398 TCS longitudinal profiles.

3 Results

The BEV and PHEV were simulated to determine battery wear rates under the conditions outlined in Table 4.

Table 4. Tested wear conditions for the BEV and PHEV.

BEV	PHEV
Distribution of U.S. ambient conditions (Portland, ME to Honolulu, HI)	Distribution of U.S. ambient conditions (Portland, ME to Honolulu, HI)
Range of max allowable DoD (80%–94%)	Range of max allowable DoD (55%–87%)
Range of VMT (398 TCS profiles)	Range of CD VMT (398 TCS profiles)

3.1 Battery Electric Vehicle

3.1.1 U.S. Ambient Conditions

Figure 8 and Figure 9 show resistance growth and capacity loss distributions after 8 years of wear for the BEV subject to U.S. ambient temperatures and U.S. average driving distributions. Resistance growth ranges from 12% to 26% while capacity loss ranges from 20% to 32% subject to ambient conditions.

Wear rate variability is strongly linked to battery temperature variability. Figure 10 shows the distribution of yearly average battery temperatures experienced by the BEV. Pack temperature in the BEV was found to be greater than or equal to the ambient temperature in the absence of an active

TMS. The BEV battery pack is heated above ambient due to solar loading and internal heat generation during driving and charging.

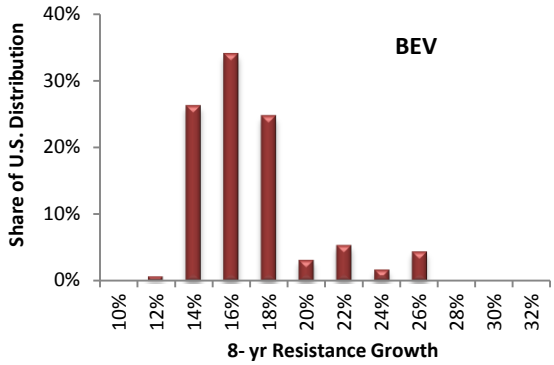

Figure 8. Weighted distribution of 8-year resistance growth for BEV exposed to 100 U.S. ambient conditions and NHTS national driving distribution.

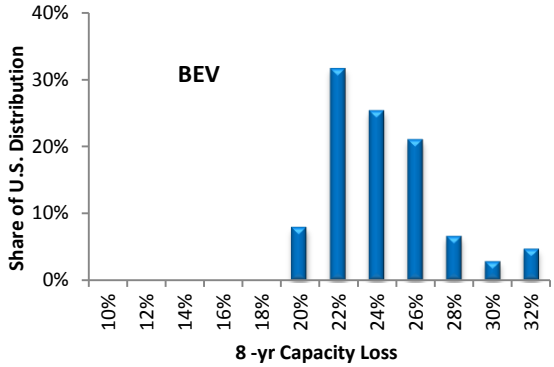

Figure 9. Weighted distribution of 8-year capacity loss for BEV exposed to 100 U.S. ambient conditions and NHTS national average driving distribution.

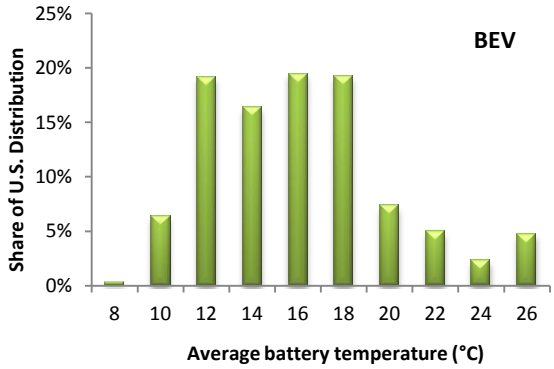

Figure 10. Weighted distribution of average yearly battery temperature for BEV exposed to 100 U.S. ambient conditions and NHTS national average driving distribution.

3.1.2 Depth of Discharge

Battery wear rate is sensitive to both maximum DoD and maximum SOC allowed by the battery management system. This sensitivity was explored using the life model by simulating wear rates for a number of battery sizes in the BEV architecture. All battery sizes allowed the vehicle to discharge 21.6 kWh of energy from the battery and achieved consistent range, acceleration, and efficiency values to within ±1% of the nominal vehicle design. Figure 11 shows resistance growth and capacity loss at 8 years for multiple battery sizes subject to ambient conditions in Los Angeles, CA.

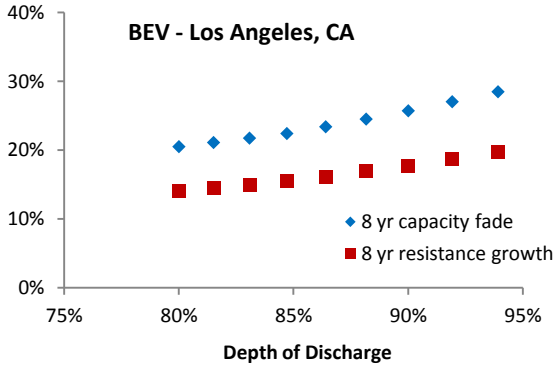

Figure 11. Eight-year resistance growth and capacity fade as a function of maximum allowable DoD for BEV exposed to ambient conditions in Los Angeles, CA and NHTS national driving distribution.

As expected, wear can be seen to increase as the maximum allowable DoD window is expanded to maintain range for smaller battery packs. Increasing the maximum allowable DoD of the pack from 80% to 94% causes 8-year resistance growth and capacity fade values to increase by 6% and 8% respectively. Using near-term battery prices ($700/kWh production cost [16]) the 94% DoD scenario represents a beginning-of-life pack cost savings of $700 while the 80% DoD design increases cost by $2,100 (both relative to the 90% DoD pack).

3.1.3 Vehicle Miles Traveled

Battery wear in the BEV was subjected to 398 longitudinal distance distributions as interpreted from the TCS. Figure 12 shows the results of this simulation in terms of resistance growth and capacity fade after 8 years subject to ambient conditions in Los Angeles, CA.

Increased VMT can be seen to have opposing effects on resistance growth and capacity loss in the BEV for the simulated longitudinal profiles. Eight-year resistance growth increases by 18% over the selected range of VMT while capacity fade actually decreases by 5% at high VMT.

In the life model, capacity fade is dictated by the greater of two fade mechanisms, calendar and cycling. In this case, calendar fade is the dominant mechanism driven by average daily voltage. By increasing VMT, the battery is allowed to spend greater amounts of time resting at lower voltages (before daily recharge), which extends calendar life and thus reduces capacity fade.

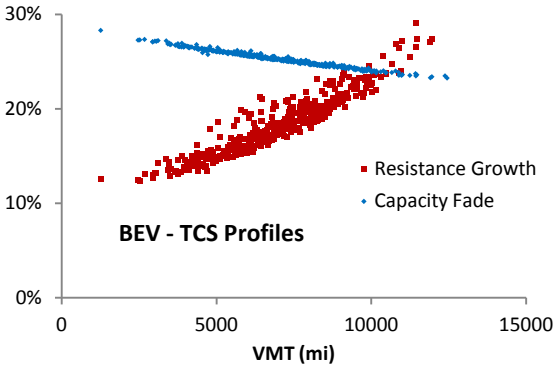

Figure 12. Eight-year resistance growth and capacity fade as a function of VMT for BEV exposed to ambient conditions in Los Angeles, CA and 398 longitudinal driving distributions.

This analysis is restricted to the single-charge-per-day scenario, and as such, driving days with distances longer than the nominal range of the vehicle are assumed to be accommodated by an alternative means of transportation. To represent the percentage of annual miles the BEV can achieve relative its original distribution, a BEV-specific, multiple day individual utility factor (IUF_{BEV}) is implemented according to Equation 5. As an example, a longitudinal distribution with an IUF_{BEV} equal to 50% would be able to achieve half of its annual miles in the BEV with one charge per day with the remaining miles accommodated by some other means.

$$IUF_{BEV} = \frac{Achieved\ Annual\ Miles}{Annual\ Miles\ of\ Original\ Distribution} \quad (5)$$

A unique IUF_{BEV} is calculated for each of the 398 longitudinal profiles. The distribution of IUF_{BEV} for the TCS is shown in Figure 13. The minimum and maximum of this distribution are 3% and 100%, respectively, with the mean occurring at an IUF_{BEV} of 75%.

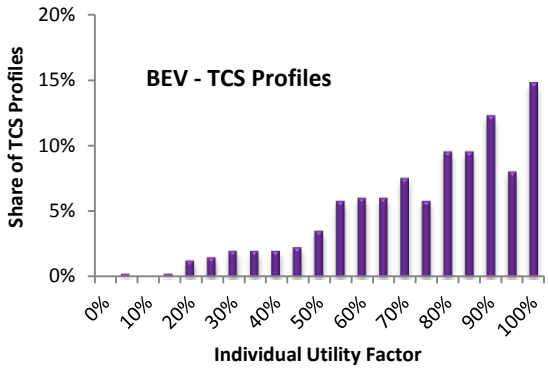

Figure 13. Distribution of IUF for BEV exposed to ambient conditions in Los Angeles, CA and 398 longitudinal driving distributions over 8 years.

3.2 Plug-In Hybrid Electric Vehicle

3.2.1 U.S. Ambient Conditions

Resistance growth and capacity fade distributions after 8 years of use for the PHEV subject to U.S. ambient temperatures and average driving distributions can be seen in Figure 14 and Figure 15. Resistance growth ranges from 18%–26%, and capacity loss ranges from 14%–20% over 8 years subject to variation in ambient temperature.

Figure 16 shows the distribution of battery temperatures experienced by the PHEV when exposed to U.S. ambient conditions. By reducing average battery temperatures and minimizing the effect of ambient conditions on the battery, the active TMS in the PHEV allows for reduced wear rates with relatively low amounts of variability with respect to regional climate differences experienced in the United States.

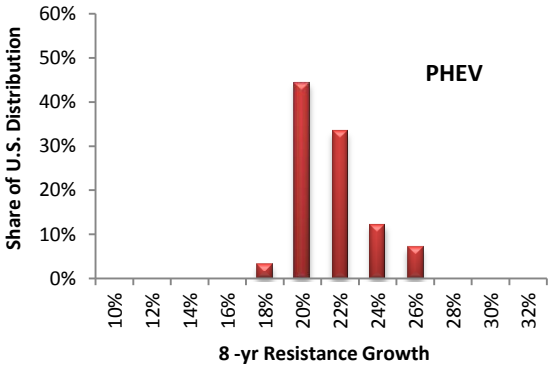

Figure 14. Weighted distribution of 8-year resistance growth for PHEV exposed to 100 U.S. ambient conditions and NHTS national driving distribution.

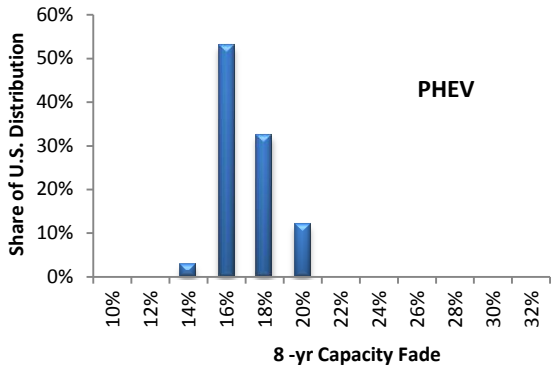

Figure 15. Weighted distribution of 8-year capacity fade for PHEV exposed to 100 U.S. ambient conditions and NHTS national driving distribution.

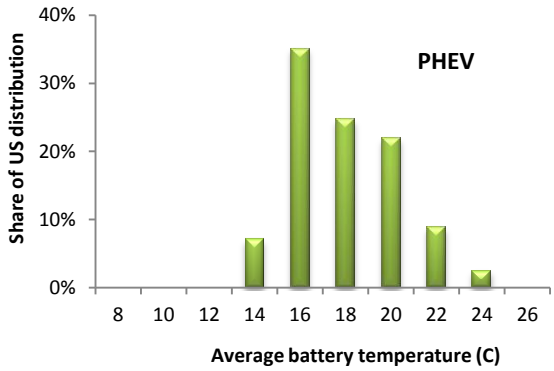

Figure 16. Weighted distribution of average yearly battery temperature for PHEV exposed to 100 U.S. ambient conditions and NHTS national driving distribution.

3.2.2 Depth of Discharge

Battery wear sensitivity to maximum allowable DoD was explored for the PHEV. All battery sizes allowed the vehicle to discharge 10.4 kWh of energy from the battery and achieved consistent CD range, acceleration, and efficiency values to within ±1% of the baseline case. Figure 17 shows resistance growth and capacity loss at 8 years for a range of battery sizes.

Increasing the maximum allowable DoD window of the PHEV from 55% to 87% increased resistance growth by 18% while capacity loss increased by 8% over the same range. As the maximum allowable DoD window is expanded, increased resistance growth limits the power capability of the pack. Loss of pack power would be reflected at the vehicle level in an increased degree of blended electric/petroleum operation or reduced all-electric vehicle power. The 87% DoD scenario represents a beginning-of-life pack cost savings of $2,800 while the 55% DoD design increases cost by $2,100 (both relative to the 65% DoD pack).

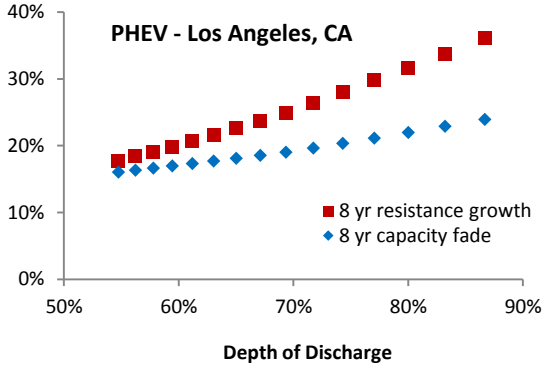

Figure 17. 8-year resistance growth and capacity fade as a function of maximum allowable DoD for PHEV exposed to ambient conditions in Los Angeles, CA and NHTS national driving distribution.

3.2.3 Vehicle Miles Traveled

The PHEV was subjected to an array of annual VMT scenarios according to the 398 longitudinal profiles derived from the TCS. Figure 18 shows the results of this analysis in terms of resistance growth and capacity fade after 8 years subject to ambient conditions in Los Angeles, CA.

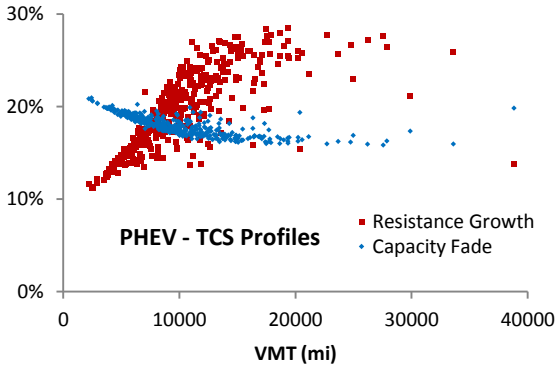

Figure 18. 8-year resistance growth and capacity loss as a function of VMT for PHEV exposed to ambient conditions in Los Angeles, CA and 398 longitudinal driving distributions.

As with the BEV, increased VMT can be seen to have opposing effects on resistance growth and capacity loss. Eight-year resistance growth increases by 17% over the selected range of VMT while capacity fade decreases by 5% at high VMT.

Note that the scatter of resistance growth and capacity fade is not as strongly correlated to VMT as was the BEV. This is due to the discrepancy in wear mechanisms between CD and CS operation in the PHEV. Wear induced by the deep cycles of CD operation significantly outweigh battery

degradation associated with the shallow cycling of CS operation. Battery wear in the PHEV can be seen to be more closely related with CD VMT, as shown in Figure 19.

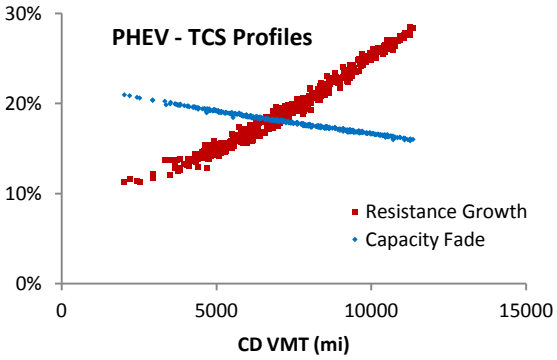

Figure 19. 8-year resistance growth and capacity fade as a function of CD VMT for PHEV exposed to ambient conditions in Los Angeles, CA and 398 longitudinal distributions.

A unique IUF is again calculated for each of the 398 longitudinal profiles. However, since the PHEV is assumed to have access to refueling stations, allowing it to operate in CS mode for a nearly unlimited distance, IUF_{PHEV} is calculated as the ratio of annual miles achieved in CD mode to the total annual miles (see Equation 6). For example, a distribution with an IUF_{PHEV} equal to 50% would be able to achieve half of its annual miles in CD mode (with one charge per day) with the remaining miles accomplished with the PHEV in CS mode.

$$IUF_{PHEV} = \frac{Annual\ CD\ Miles}{Annual\ CD + Annual\ CS\ Miles} \quad (6)$$

The distribution of IUF_{PHEV} for the TCS is shown in Figure 20. The minimum and maximum of this distribution are 9% and 100%, respectively, with the mean occurring at an IUF_{PHEV} of 78%.

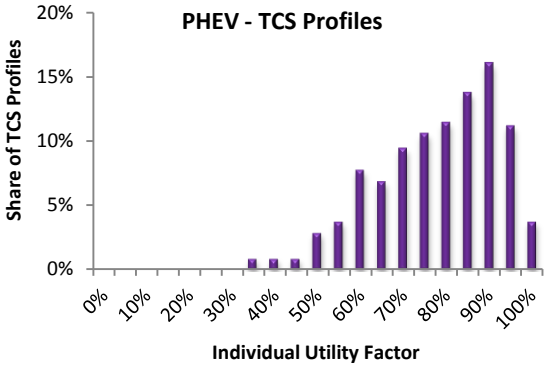

Figure 20. Distribution of IUF for PHEV exposed to ambient conditions in Los Angeles, CA and 398 longitudinal driving distributions over 8 years.

4 Conclusions

The sensitivity of battery wear to ambient conditions, battery size, and usage patterns has been explored. Major results of this analysis include:

- The spectrum of climate and usage conditions PEVs are expected to face in the U.S. market suggest that the assumption of a single average ambient condition for battery wear calculations may not be representative of observed behavior in the fleet.

- Ambient conditions have a large effect on battery wear for all variables considered in this study. The effects of ambient conditions on battery life can be mitigated by appropriate vehicle design. Thermal insulation and TMSs can be designed to improve fade rates for each vehicle platform.

- TMSs that employ active battery heating/ cooling can reduce the amount of temperature variability in the pack. The passively cooled BEV experienced yearly average pack temperatures from 8°C to 26°C while the actively heated/cooled PHEV ranged from 14°C to 24°C.

- Maximum allowable DoD was found to significantly impact battery wear. Resistance growth and capacity fade were significantly reduced by designing a pack to operate with a relatively low maximum allowable DoD. However, pack design for low DoD can increase up-front vehicle costs by requiring additional total energy to achieve a desired CD range. For the modeled BEV, the extra battery capacity required for an 80% vs. 94% DoD window represents a roughly $2,800 increment in pack cost. For the modeled PHEV, the extra battery capacity required for a 55% vs. 87% DoD window represents a roughly $4,900 increment in pack cost. Increased battery energy may also require components such as the electric motor to be resized to maintain vehicle acceleration.

- The effect of VMT was explored for both the simulated BEV and PHEV. Battery wear was found to be a strong function of VMT for the BEV and of CD VMT for the PHEV. Under the single-charge-per-day assumption, increasing VMT was observed to decrease

capacity fade as longer driving trips reduced the amount of high voltage exposure to which the pack was subjected. This effect is believed to be pronounced by the unique characteristics of the NCA chemistry and would be expected to change significantly under alternative charge strategies (just-in-time, end-of-day, opportunity, 1x/day, 2x/day, etc.).

- The PHEV can achieve a comparable distribution of IUF to the BEV over 8 years despite the substantially shorter CD range of the PHEV. For the 398 longitudinal distributions simulated, the BEV achieved an average IUF of 75% compared to an average of 78% for the PHEV. This result is a product of the assumption that driving trips longer than the range of the BEV will be accommodated by some other means of transportation. The effects of this assumption are magnified as the BEV experiences reduced range due to capacity loss.

Future work may focus on improving the comparison of vehicle utility by incorporating effects of temperature on pack internal resistance and capacity. These effects are expected to reduce the utility of both BEVs and PHEVs as vehicle range is compromised at low pack temperatures and internal resistance increases at high temperatures. Additional analysis may also seek to develop a range of potential near term vehicle-to-grid scenarios to determine the subsequent impact on battery wear and achievable VMT.

Acknowledgements

The authors gratefully acknowledge the programmatic support of the U.S. Department of Energy, Office of Energy Efficiency and Renewable Energy, Vehicle Technologies Program. The authors particularly wish to thank Vehicle Systems activity managers David Anderson and Lee Slezak for their guidance and support.

References

[1] Smith, K., Markel, T., Kim, G.H., Pesaran, A., "Design of Electric Drive Vehicle Batteries for Long Life and Low Cost," National Renewable Energy Laboratory, Golden, CO, 2010, NREL/PR-540-48933.

[2] Idaho National Laboratory, "Technology Life Verification Testing," Idaho Falls, ID, 2010, INEEL-EXT-04-01986.

[3] Broussely, M., "Aging of Li-ion batteries and life prediction, an update," 3rd Int. Symposium on Large Lithium-Ion Battery Technology and Application, Long Beach, California, May 2007.

[4] Hall, J., Lin, T., Brown, G., Biensan, P., and Bonhomme, F., "Decay processes and life predictions for lithium ion satellite cells," 4th Int. Energy Conversion Engineering Conf., San Diego, California, June 2006.

[5] Smart, M., Chin, K., Whitcanack, L., and Ratnakumar, B., "Storage characteristics of Li-ion batteries," NASA Battery Workshop, Huntsville, Alabama, Nov. 2006.

[6] Broussely, M., Chap. 13 in: Advances in Lithium-Ion Batteries, van Schalkwijk, W., and Scrosati, B., editors. New York: Kluwer Academic / Plenum Publishers, 2002.

[7] Smith, K., Neubauer, J., Earleywine, M., Wood, E., and Pesaran, A., "Comparison of Plug-In Hybrid Electric Vehicle Battery Life across Geographies and Drive-Cycles," Society of Automotive Engineers 2012 World Congress, 12PFL-0731.

[8] CarsDirect, Nissan Leaf Specifications, http://www.carsdirect.com/nissan/leaf/specs, retrieved on 8-25-11.

[9] GM Volt Specifications, http://gm-volt.com/full-specifications/, retrvd. 8-25-11.

[10] National Renewable Energy Laboratory Strategic Initiative Working Group Report: Thermal Model of Gen 2 Toyota Prius, Kandler Smith, Ahnvu Le, Larry Chaney.

[11] Barnitt, R.A., Brooker, A.D., Ramroth, L., Rugh, J., Smith, K.A., "Analysis of Off-Board Powered Thermal Preconditioning in Electric Drive Vehicles," National Renewable Energy Laboratory, Golden, CO, 2010, NREL/CP-5400-49252.

[12] R.L. Polk & Co., https://www.polk.com.

[13] National Renewable Energy Laboratory, National Solar Radiation Database, Typical Meteorological Year Database 3, Golden, CO.

[14] 2001 National Household Travel Survey, http://nhts.ornl.gov/.

[15] National Renewable Energy Laboratory, Center for Transportation and Technology Systems, Transportation Secure Data Center: http://www.nrel.gov/vehiclesandfuels/secure_transportation_data.html.

[16] U.S. Department of Energy, Vehicle Technologies Program, 2011 Annual Merit Review and Peer Evaluation Meeting, Energy Storage R&D, May 2011.

Authors

Eric Wood
National Renewable Energy Lab
Golden, Colorado USA
Email: eric.wood@nrel.gov

Mr. Wood is an Engineer at NREL's Center for Transportation Technologies and Systems. He holds a B.S. in Mechanical Engineering from the University of Nebraska (2009) and a M.S. in Mechanical Engineering from Colorado State University (2011).

Jeremy Neubauer
National Renewable Energy Lab
Golden, Colorado USA
Email: jeremy.neubauer@nrel.gov

Dr. Jeremy Neubauer is a Senior Engineer with NREL's Center for Transportation Technologies and Systems, where his primary responsibility lies in researching the reuse of retired automotive traction batteries and modeling the total cost of ownership of advanced vehicle types. Prior to coming to NREL, Dr. Neubauer was Chief Engineer at ABSL Space Products, a leading manufacturer of Li-Ion batteries for the space industry. Dr. Neubauer has a Bachelors, Masters, and Doctorate in Mechanical Engineering from Washington University in St. Louis.

Aaron D. Brooker
National Renewable Energy Lab
Golden, Colorado USA
Email: aaron.brooker@nrel.gov

Mr. Brooker is a Senior Engineer at NREL. He holds a B.S. in Mechanical Engineering from Michigan Technological University (1998) and an M.S. in Mechanical Engineering from the University of Colorado (2000).

Jeffrey Gonder
National Renewable Energy Laboratory
Golden, Colorado USA
Email: jeff.gonder@nrel.gov

Mr. Gonder is a Senior Engineer at NREL's Center for Transportation Technologies and Systems. He holds a B.S. in Mechanical Engineering from the University of Colorado and an M.S. in Mechanical Engineering from Pennsylvania State University. His research activities include both simulation and hardware testing of conventional, hybrid, plug-in and fuel cell vehicles.

Kandler A. Smith
National Renewable Energy Lab
Golden, Colorado USA
Email: kandler.smith@nrel.gov

Dr. Smith is a Senior Engineer researching energy storage systems for NREL's Center for Transportation Technologies and Systems. He holds a Ph.D. degree in Mechanical Engineering from Pennsylvania State University. He is an active member of the IEEE, the Electrochemical Society, and the Society for Automotive Engineers. His research includes electric-drive vehicles, battery electrochemical/ thermal characterization and modeling, and battery-life predictive modeling.

List of Acronyms

BEV	battery electric vehicle
CD	charge depleting
CS	charge sustaining
DoD	depth of discharge
FASTSim	Future Automotive Systems Technology Simulator
HEV	hybrid electric vehicle
IUF	individual utility factor
LA92	California Air Resources Board Unified Driving Schedule
Li	lithium
NCA	nickel-cobalt-aluminum
NHTS	National Household Travel Survey
NREL	National Renewable Energy Laboratory
PEV	plug-in electric vehicle
PHEV	plug-in hybrid electric vehicle
TCS	Traffic Choices Study
TMS	thermal management system
TMY3	Typical Meteorological Year Database
UDDS	Urban Dynamometer Driving Schedule
US06	Supplemental Federal Test Procedure Driving Schedule
VMT	vehicle miles traveled